IL NUOVO CIMENTO Vol. 35 C, N. 1 Gennaio-Febbraio 2012
DOI 10.1393/ncc/i2012-11151-7

Colloquia: LaThuile11

The Planck mission: From first results to cosmology

P. Natoli([1])([2])([3]), C. Burigana([3]), A. Gruppuso([3]) and N. Mandolesi([3])

([1]) *Dipartimento di Fisica, Università degli Studi di Ferrara - via Giuseppe Saragat 1 I-44100 Ferrara, Italy*

([2]) *Agenzia Spaziale Italiana Science Data Center, c/o ESRIN - via Galileo Galilei Frascati, Italy*

([3]) *INAF-IASF Bologna, Istituto di Astrofisica Spaziale e Fisica Cosmica di Bologna Istituto Nazionale di Astrofisica - via Piero Gobetti 101, I-40129 Bologna, Italy*

(ricevuto il 29 Settembre 2011; pubblicato online il 25 Gennaio 2012)

Summary. — *Planck* is a ESA satellite, currently in operation, whose main objective is to accurately image the anisotropies of the Cosmic Microwave Background Radiation in intensity and polarization. Benefiting from an unprecedented combination of sensitivity, angular resolution, and frequency leverage, *Planck* will provide high quality data to be mined in cosmology and astrophysics. The first Planck results have been released in January 2011 and include both Galactic and extragalactic source catalogues, a list of galaxy clusters selected by the Sunyaev-Zel'dovich effect, and a cold cores catalogue. The first cosmological data products are awaited for early 2013. *Planck* has a wide list of scientific targets. Here we focus on one specific aspect which is also of interest to the high energy physics community: constraining the Parity and $\mathcal{CPT}$ symmetries through CMB datasets. We describe the basic formalism, the relevant estimators and the overall analysis strategy. We provide marginal evidence for large scale Parity anomaly in the WMAP data that may be soon confirmed or discarded by the *Planck* satellite. *Planck* is currently measuring CMB anisotropies and their polarization with a level of precision that will remain unparalleled for many years to come. We also show how the CMB can be used to constrain fundamental symmetry violations in the photon sector through the so-called cosmological birefringence phenomenon.

PACS 98.80.-k – Cosmology.

© Società Italiana di Fisica

1. – Introduction

Planck([1]), is the third generation mission devoted to the Cosmic Microwave Background (CMB), after the COsmic Background Explorer (COBE) and Wilkinson Microwave Anisotropy Probe (WMAP)([2]), and at the fronteer of precision cosmology today [1-3]. It is equipped with a 1.5–m effective aperture telescope with two actively-cooled instruments observing the sky in nine frequency bands from 30 GHz to 857 GHz: the Low Frequency Instrument (LFI) operating at 20 K with pseudo-correlation radiometers, and the High Frequency Instrument (HFI) with bolometers operating at 100 mK. A summary of the LFI and HFI performances is reported in table I. *Planck* is sensitive to linear polarization up to 353 GHz. The constraints on the thermal behavior, required to minimize systematic effects, resulted in a cryogenic architecture that is one of the most complicated ever conceived for space. Moreover, the spacecraft has been designed to exploit the favorable thermal conditions of the orbit around the second Lagrangian point of the Sun-Earth system. *Planck* is a spinning satellite. Thus, its receivers will observe the sky through a sequence of (almost great) circles following a scanning strategy aimed at minimizing systematic effects and achieving all-sky coverage for all receivers [4].

After launch on 14 May 2009, *Planck* has already mapped the sky about four times (at the time of writing this proceedings paper) and it is planned to complete another full sky survey with both instrument operational, and yet another one for LFI only. The HFI is expected to reach end of life after the end of the fifth sky survey, due to cryogenic helium consumption.

The first scientific results of *Planck* have been released on January 2011 [6]. They describe the instrument performance in flight including thermal behaviour [7-9], the HFI and LFI data analysis pipelines [10,11], the main astrophysical results about Galactic science [12-18], extragalactic sources and far-IR background [19-24], and Sunyaev-Zel'dovich effects and cluster properties [25-29], providing to the scientific community the *Planck* Early Release Compact Source Catalog (ERCSC) [30]. The first publications of the main cosmological implications are expected in early 2013.

The anisotropy pattern of the CMB, measured by WMAP, probes cosmology with unprecedented precision (see [31, 32] and references therein). WMAP data are largely consistent with the concordance Λ cold dark matter (ΛCDM) model, but there are some interesting deviations from it, in particular on the largest angular scales [33]. See also [34] for a critical point of view upon the subject.

A large number of papers dealing with these anomalies have been published in the last years. We briefly list below those that are the most studied: a) lack of power on large angular scales [35,36]; b) hemispherical asymmetries [37-43]; c) unlikely alignments of low multipoles [44-48, 35, 49-53]; d) non-Gaussianity [43, 54, 55]; e) spots and/or excess of signal [56, 57, 42], possibly linked to non-Gaussianity; f) Parity asymmetry. This anomaly represents one subject of the present paper. It has been suggested in [58] that an estimator built upon the point Parity symmetry might be used as a practical tool for detecting foregrounds. In particular these authors consider whether the observed

([1]) `http://www.esa.int/Planck`. is a project of the European Space Agency—ESA—with instruments provided by two scientific Consortia funded by ESA member states (with France and Italy as lead countries), contributions from NASA (USA), and telescope reflectors provided in a collaboration between ESA and a scientific Consortium led and funded by Denmark.
([2]) `http://lambda.gsfc.nasa.gov/`

TABLE I. – *Planck performances. The average sensitivity, $\delta T/T$, per $FWHM^2$ resolution element (FWHM is reported in arcmin) is given in CMB temperature units (i.e. equivalent thermodynamic temperature) for* 28 *months of integration. The white noise (per frequency channel for LFI and per detector for HFI) in* 1 *sec of integration (NET, in $\mu K \cdot \sqrt{s}$) is also given in CMB temperature units. The other used acronyms are: DT = detector technology, N of R (or B) = number of radiometers (or bolometers), EB = effective bandwidth (in GHz). Adapted from* [5, 2] *and* [3].

LFI			
Frequency (GHz)	30	44	70
InP DT	MIC	MIC	MMIC
FWHM	33.34	26.81	13.03
N of R (or feeds)	4 (2)	6 (3)	12 (6)
EB	6	8.8	14
NET	159	197	158
δT/T [μK/K] (in T)	2.48	3.82	6.30
δT/T [μK/K] (in P)	3.51	5.40	8.91
HFI			
Frequency (GHz)	100		143
FWHM in T (P)	(9.6)		7.1 (6.9)
N of B in T (P)	(8)		4 (8)
EB in T (P)	(33)		43 (46)
NET in T (P)	100 (100)		62 (82)
δT/T [μK/K] in T (P)	2.1 (3.4)		1.6 (2.9)
Frequency (GHz)	217		353
FWHM in T (P)	4.6 (4.6)		4.7 (4.6)
N of B in T (P)	4 (8)		4 (8)
EB in T (P)	72 (63)		99 (102)
NET in T (P)	91 (132)		277 (404)
δT/T [μK/K] in T (P)	3.4 (6.4)		14.1 (26.9)
Frequency (GHz)	545		857
FWHM in T	4.7		4.3
N of B in T	4		4
EB in T	169		257
NET in T	2000		91000
δT/T [μK/K] in T	106		4243

low CMB quadrupole in temperature could more generally signal odd point-Parity, *i.e.* suppression of even multipoles. However they claim that WMAP dataset never supports Parity preference beyond the meagre 95% confidence level. Later, [59] found that the Parity symmetry in the temperature map of WMAP 3 and 5 year data is anomalous at the level of 4 out of 1000 in the range $\delta\ell = [2, 18]$. This analysis have been repeated in the WMAP 7 year data confirming the anomaly at same level for a slightly wider range $\delta\ell = [2, 22]$ [60]. We report in this paper that analysis and its extension to polarization [61]. In fact, the CMB polarization pattern can provide information on symmetry-violating physics beyond the standard model.

In general, the breakdown of spacetime symmetries is a potential tracer of new physics [62]. Several models exist that predict non-standard $\mathcal{P}$ and $\mathcal{CP}$ violations ("$\mathcal{C}$" standing for charge conjugation), as well as $\mathcal{CPT}$ violations ("$\mathcal{T}$" being time reversal) and the related (through the anti-$\mathcal{CPT}$ theorem [63, 64]) breakdown of Lorentz invariance. A number of tests have been suggested and (in many cases) performed, either in terrestrial and orbital laboratories [65, 66] or through cosmological observations [67-69]. These violations may also be seen as anomalies the CMB polarization pattern, since its statistical properties are constrained by the assumption of symmetry conservation.

The paper is organized as follows. In sect. **2** we describe the basic formalism, the performed analysis, and the relevant symmetry estimators. Current results on symmetry estimators based on WMAP data are given in sect. **3** while in sect. **4** we focus on the implications for birefringence. The forecasts for *Planck* about these topics are provided in sect. **5**. The precise extraction of the cosmological information from microwave observations requires an extremely accurate and efficient data analysis and a careful separation of CMB and astrophysical emissions (see, *e.g.*, [70] for a discussion of this topics in the context of the *Planck* surveys). Finally, our conclusions are drawn in sect. **6**.

2. – Description of the analysis

2˙1. *Introduction.* – All-sky temperature maps, $T(\hat{n})$, are usually expanded in Spherical Harmonics $Y_{\ell m}(\hat{n})$, with $\hat{n}$ being a direction in the sky, namely depending on the couple of angles (θ, ϕ):

$$a_{T,\ell m} = \int \mathrm{d}\Omega\, Y^{\star}_{\ell m}(\hat{n})\, T(\hat{n}), \tag{1}$$

where $a_{T,\ell m}$ are the coefficients of the Spherical Harmonics expansion and $\mathrm{d}\Omega = \mathrm{d}\theta\mathrm{d}\phi \sin\theta$. Under reflection (or Parity) symmetry ($\hat{n} \to -\hat{n}$), these coefficients behave as

$$a_{T,\ell m} \to (-1)^{\ell}\, a_{T,\ell m}\,. \tag{2}$$

Analogously for polarizations maps, taking into account the usual combination of Stokes parameters ($Q(\hat{n})$ and $U(\hat{n})$)

$$a_{\pm 2,\ell m} = \int \mathrm{d}\Omega\, Y^{\star}_{\pm 2,\ell m}(\hat{n})\, (Q(\hat{n}) \pm iU(\hat{n})), \tag{3}$$

where $Y_{\pm 2,\ell m}(\hat{n})$ are the Spherical Harmonics of spin 2 and $a_{\pm 2,\ell m}$ are the corresponding

coefficients, it is possible to show that under Parity

$$a_{E,\ell m} \to (-1)^{\ell}\, a_{E,\ell m}, \tag{4}$$

$$a_{B,\ell m} \to (-1)^{\ell+1}\, a_{B,\ell m}, \tag{5}$$

where

$$a_{E,\ell m} = -(a_{2,\ell m} + a_{-2,\ell m})/2, \tag{6}$$

$$a_{B,\ell m} = -(a_{2,\ell m} - a_{-2,\ell m})/2i. \tag{7}$$

Equations (2), (4) and (5) show that the cross-correlations $C_\ell^{TB} = C_\ell^{EB} = 0$.

Further details can be found for example in [71], [72] and explicit algebra is present in the Appendix of [61].

In order to evaluate the angular power spectrum (APS) we adopt the quadratic maximum likelihood (QML) estimator, introduced in [73] and extended to polarization in [74]. Further details can be found in [75].

2˙2. *Angular power spectrum estimation, data set and simulations.* – In order to evaluate the angular power spectrum (APS) we adopt the quadratic maximum likelihood (QML) estimator, introduced in [73] and extended to polarization in [74]. Further details can be found in [75]. Now, we describe the data set that we have considered. We use the temperature ILC map smoothed at 9.8 degrees and reconstructed at HEALPix([3]) [76] resolution $N_{side} = 16$, the foreground cleaned low resolution maps and the noise covariance matrix in (Q, U) publicly available at the Legacy Archive for Microwave Background Data Analysis (LAMBDA) website([4]) for the frequency channels Ka, Q and V as considered by [31] for the low ℓ analysis. These frequency channels have been co-added as follows [77]:

$$m_{tot} = C_{tot}\left(C_{Ka}^{-1} m_{Ka} + C_Q^{-1} m_Q + C_V^{-1} m_V\right), \tag{8}$$

where m_i, C_i are the polarization maps and covariances (for $i =$ Ka, Q and V) and

$$C_{tot}^{-1} = C_{Ka}^{-1} + C_Q^{-1} + C_V^{-1}. \tag{9}$$

This polarization data set has been extended to temperature considering the ILC map. We have added to the temperature map a random noise realization with variance of $1\,\mu\mathrm{K}^2$ as suggested in [78]. Consistently, the noise covariance matrix for TT is taken to be diagonal with variance equal to $1\,\mu\mathrm{K}^2$.

We have also performed Monte-Carlo simulations in order to assess the significance of our results. A set of 10000 CMB + noise sky realizations has been generated: the signal extracted from the WMAP 7 years best fit model, the noise through a Cholesky decomposition of the noise covariance matrix. We have then computed the APS for each of the 10000 simulations by means of *BolPol* and build two figures of merit as explained in the next subsection.

([3]) `http://healpix.jpl.nasa.gov/`
([4]) `http://lambda.gsfc.nasa.gov/`

2˙3. *Estimators*. – We define the following quantities:

$$C^X_{+/-} \equiv \frac{1}{(\ell_{max}-1)} \sum_{\ell=2,\ell_{max}}^{+/-} \ell(\ell+1) 2\pi \hat{C}^X_\ell, \tag{10}$$

where $\hat{C}^X_\ell$ are the estimated APS obtained with the *BolPol* code [75] for the power spectrum X = TT, TE, EE and BB. The sum is meant only over the even or odd ℓ (and this is represented respectively by the symbol + or −) with $\ell_{max} \geq 3$.

Therefore, two estimators can be built from eq. (10) as follows: the ratio R^X, as performed in [59] or [60],

$$R^X = C^X_+ / C^X_-, \tag{11}$$

and, in analogy to what performed for the hemispherical symmetry in [41], the difference D^X

$$D^X = C^X_+ - C^X_-, \tag{12}$$

of the two aforementioned quantities. In the following, we drop the index X for R and D specifying every time we use them which is the spectrum they refer to.

For our application to WMAP data, both estimators have been considered for the TT spectrum but only the second one for the other spectra (EE, TE and BB). This is due the unfavorable signal-to-noise ratio of the WMAP data in polarization.

For X = TB and EB we simply use the average power

$$C^X \equiv \frac{1}{(\ell_{max}-1)} \sum_{\ell=2,\ell_{max}} \frac{\ell(\ell+1)}{2\pi} \hat{C}^X_\ell. \tag{13}$$

3. – Results

In fig. 1 we show the estimator R and D for TT averaged in $\delta\ell = [2, 22]$ and in $\delta\ell = [2, 33]$. The probability to obtain a smaller value than the WMAP one is 0.47% for R in the range $\delta\ell = [2, 22]$ and 3.17% in the range $\delta\ell = [2, 33]$. For the D estimator the probability is 0.63% in the range $\delta\ell = [2, 22]$ and 3.17% in the range $\delta\ell = [2, 33]$. The upper left panel of fig. 1 recovers the same level of anomaly claimed in [60].

In fig. 2 we plot the percentage related to the WMAP 7 y Parity anomaly for TT versus ℓ_{max} in the range [10,40] for the two considered estimators. As evident there is not a single ℓ_{max} for which the TT anomaly shows up, but rather a characteristic scale, see also [60]. For the estimator of eq. (11) the percentage anomaly is well below 1% for almost any choice of ℓ_{max} in the range [15,25](5). As also shown in fig. 2, the estimator of eq. (12) follows closely the other estimator although it is slightly less sensitive. Therefore, we find a whole multipole range, rather than a single ℓ_{max} value, where the WMAP 7 y Parity anomaly holds. This dims significantly the case for posterior biasing.

(5) Only for $\ell_{max} = 21$ the estimator of eq. (11) exhibits a percentage which is of the order of 1%.

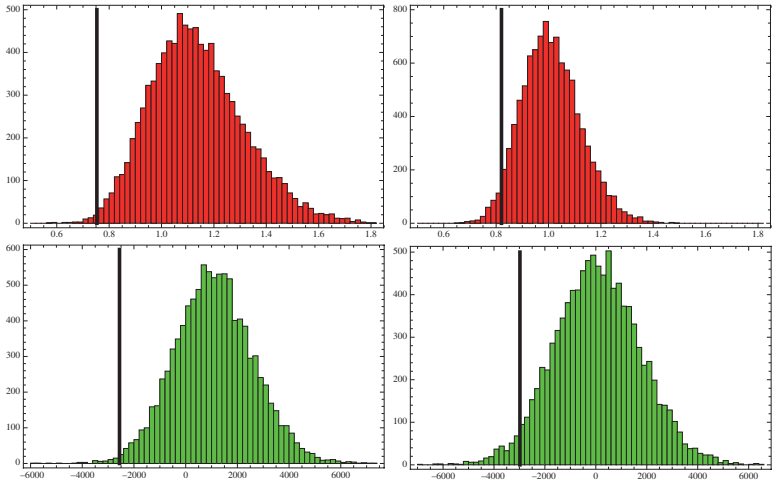

Fig. 1. – TT. Counts (y-axis) *vs.* the estimator (x-axis). Upper histograms: Ratio for the range $\delta\ell = [2, 22]$ (left panel) and for the range $\delta\ell = [2, 33]$ (right panel). Lower histograms: Difference for the range $\delta\ell = [2, 22]$ (left panel) and for the range $\delta\ell = [2, 33]$ (right panel). Units for the estimator D are $\mu\mathrm{K}^2$. The vertical line stands for the WMAP 7 year value.

In table II we provide the results for EE, TE and BB. As mentioned above, only D is considered and computed for the four following multipoles range $\delta\ell = [2, 4]$, $[2, 8]$, $[2, 16]$ and $[2, 22]$. No anomalies have been found and compatibility with Parity symmetry is obtained.

In table III we provide the results for EB and TB where the estimator C is considered and computed for the same aforementioned four multipoles range. Both the spectra are well consistent with zero. Only the EB spectrum shows a mild anomaly in the range $\delta\ell = [2, 22]$ at the level of 97.7%. This is due to five estimates from $\ell = 18$ to $\ell = 22$ that

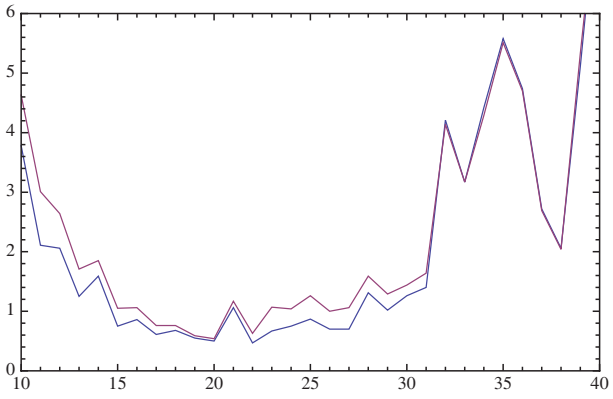

Fig. 2. – TT. Percentage of the WMAP 7 y value (y-axis) *vs.* ℓ_{max} (x-axis). Blue line is for the ratio and the red line for the difference. This analysis shows that there is no single ℓ_{max} for which the TT anomaly shows up, but rather suggests the existence of a characteristic scale, see also [60].

TABLE II. – *Probabilities (in percentage) to obtain a smaller value than the WMAP* 7 y *one.*

D	$\delta\ell = [2,4]$	$\delta\ell = [2,8]$	$\delta\ell = [2,16]$	$\delta\ell = [2,22]$
EE	93.09	76.21	44.27	46.61
TE	56.35	38.88	24.79	22.77
BB	7.97	13.42	11.70	44.31

are systematically larger than zero. When these points are excluded this mild anomaly drops. For example in the range $\delta\ell = [2,16]$ the probability to obtain a smaller value than the WMAP one is 55.35%. The latter two estimators are shown in fig. 3.

4. – Birefringence

As shown above, if the physics controlling CMB fluctuations is Parity conserving then the cross spectra C_l^{TB} and C_l^{EB} must vanish due to the different handedness of the B and (T, E) harmonics. Therefore, if the standard cosmological model holds, we should expect no relevant information from TB and EB. On the other hand, detection of non-zero primordial TB and/or EB may probe fundamental physics in the early universe, such as the presence of a primordial homogeneous [79] or helical [80, 81] magnetic field which would induce Faraday rotation and non-zero TB correlations. Parity-asymmetric gravity dynamics during inflation may generate a discrepancy among left and right-handed gravitational waves, so that TB and EB are non-zero [82, 83]. Particle physics models with non-standard Parity-violating interactions also predict non-vanishing TB and EB signals [84-86].

In this section we focus on a class of models that exhibit Parity violations in the photon sector [87]. A Chern-Simons term can be introduced in the effective Lagrangian [68, 69]:

$$\Delta\mathcal{L} = -\frac{1}{4}\, p_\mu \epsilon^{\mu\nu\rho\sigma} F_{\rho\sigma} A_\nu,$$

where $F^{\mu\nu}$ is the Maxwell tensor and A^μ the 4-potential. The 4-vector p_μ may be interpreted as the derivative of the quintessence field or the gradient of a function of the Ricci scalar [88,89]. In either case a $\mathcal{P}$ violation always arises provided that p_0 is non-zero, while $\mathcal{C}$ and $\mathcal{T}$ remain intact. Hence, $\mathcal{CP}$ and $\mathcal{CPT}$ symmetries are also violated, as well as Lorentz invariance, since p^μ picks up a preferred direction in space-time. The net effect on a propagating photon is to rotate its polarization direction by an angle $\Delta\alpha$, hence the name "cosmological birefringence". Historically, the effect has being constrained by measuring polarized light from high redshift radio galaxies and quasars [68, 69, 90-94].

TABLE III. – *Probabilities (in percentage) to obtain a smaller value than the WMAP* 7 y *one.*

C	$\delta\ell = [2,4]$	$\delta\ell = [2,8]$	$\delta\ell = [2,16]$	$\delta\ell = [2,22]$
TB	51.78	39.42	6.71	10.55
EB	62.73	69.83	55.35	97.70

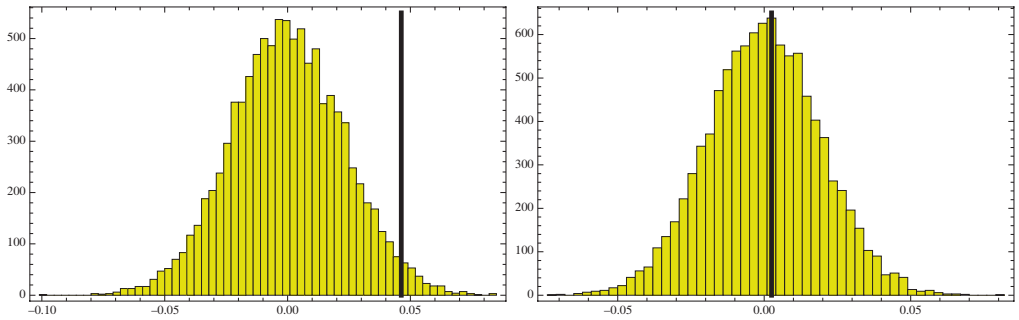

Fig. 3. – EB. Counts (y-axis) *vs.* the estimator C (x-axis). Distribution of C for $\delta\ell = [2, 22]$ (left panel) and $\delta\ell = [2, 16]$ (right panel). Units are $\mu\mathrm{K}^2$. The vertical line stands for the WMAP 7 y data.

Obviously, the CMB photons would also be affected and, due to their longer journey, may get a larger rotation. A consequence for the CMB pattern is the mixing of E and B modes: the TB and EB correlations still vanish at last scattering surface, but the observable CMB spectra are distorted as [82, 83, 95]:

$$C_l'^{TB} = C_l^{TE} \sin 2\Delta\alpha, \tag{14}$$

$$C_l'^{EB} = \frac{1}{2}\left(C_l^{EE} - C_l^{BB}\right) \sin 4\Delta\alpha, \tag{15}$$

$$C_l'^{TE} = C_l^{TE} \cos 2\Delta\alpha, \tag{16}$$

$$C_l'^{EE} = C_l^{EE} \cos^2 2\Delta\alpha + C_l^{BB} \sin^2 2\Delta\alpha, \tag{17}$$

$$C_l'^{BB} = C_l^{BB} \cos^2 2\Delta\alpha + C_l^{EE} \sin^2 2\Delta\alpha, \tag{18}$$

where the primed quantities are rotated. In [32] a limit $\Delta\alpha = 0.9° \pm 1.4°$ was derived for the multipole range $\delta\ell = [23, 800]$, whereas for $\delta\ell = [2, 23]$ they find $\Delta\alpha = -3.8° \pm 5.2°$. The reason for this distinction is that the low ℓ polarization pattern is only influenced by the reionization epoch, which happened at redshift $z \simeq 10$. The primary fluctuations at higher multipoles, on the other hand, can be traced to last scattering at $z \simeq 1100$ so the corresponding angular scales allow for a much longer journey of the CMB photons. A slightly more stringent limit based on QUaD([6]) data has been set in [96] as $\Delta\alpha = 0.83° \pm 0.94° \pm 0.5°$, the second error being systematic.

5. – Planck forecast

In this section we discuss how *Planck* will improve the present constraints on the symmetry violations discussed above. We first take into account the case of the low ℓ Parity anomaly. We then discuss briefly the case of birefringence.

5˙1. *Simulated dataset*. – We consider the white noise level for 143 GHz channel of *Planck*. As in [41], we consider the nominal sensitivity of the *Planck* 143 GHz channel,

([6]) QUaD stands for "QUEST at DASI". In turn, QUEST is "Q & U Extragalactic Survey Telescope" and DASI stands for "Degree Angular Scale Interferometer".

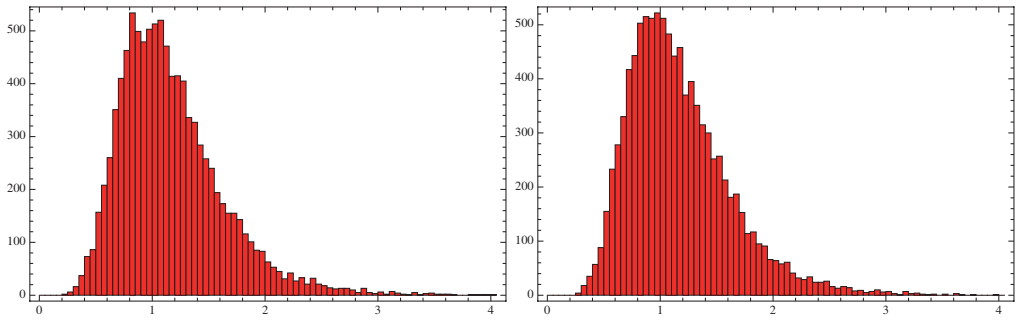

Fig. 4. – EE. Counts (y-axis) *vs.* the estimator R (x-axis). Distribution of R for $\delta\ell = [2, 22]$ (left panel) and $\delta\ell = [2, 16]$ (right panel).

taken as representative of the results which can be obtained after the foreground cleaning from various frequency channels. The 143 GHz channel has an angular resolution of $7.1'$ (FWHM) and an average sensitivity of $6\,\mu$K ($11.4\,\mu$K) per pixel—a square whose side is the FWHM size of the beam—in temperature (polarization), after 2 full sky surveys. We assume uniform uncorrelated instrumental noise and we build the corresponding diagonal covariance matrix for temperature and polarization, from which, through Cholesky decomposition we are able to extract noise realizations. For this low noise level we apply the same procedure adopted for the Monte Carlo simulations in subsect. **2**˙2.

5˙2. *Forecasts*. – From the set of 10000 CMB + noise sky realizations, we find that: The T based estimators (both R and D) do not change much since at large scale the APS for T is dominated by cosmic variance and not by the noise. For EE, TE and BB it is possible to consider even the R estimator. See for example fig. 4 where the R estimator is computed for EE in the range $\delta\ell = [2, 22]$ (left panel) and $\delta\ell = [2, 16]$ (right panel). The standard deviations for the D and C are evaluated in table IV for $\delta\ell = [2, 22]$ and compared to the WMAP 7 y ones.

The case of birefringence has been investigated in [97] where the expected standard error for *Planck* in constraining the rotation angle α is given as $\Delta\alpha = 0.057°$. Note

TABLE IV. – *Upper Table: standard deviation for the D estimator computed in the range* $\delta\ell = [2, 22]$. *Lower Table: standard deviation for the C estimator computed in the range* $\delta\ell = [2, 22]$. *Units are* $\mu\mathrm{K}^2$.

σ_D	WMAP 7 y	*Planck*
TT	1517.17	1509.21
TE	20.19	9.08
EE	0.65	0.10
BB	0.69	0.04

σ_C	WMAP 7 y	*Planck*
TB	0.95	0.19
EB	0.023	0.001

however that this error purely considers the noise level. Realistic measurements of α may be affected by systematic errors, especially arising from the uncertainties in the orientation of the polarimeters. The latter need to be properly taken into account [98].

6. – Conclusions

The *Planck* satellite is measuring CMB anisotropies and their polarization with a level of precision that will remain unparalleled for many years to come. The results derived from the *Planck* dataset will set a benchmark for precision cosmology. In this paper we have focused on fundamental information that the CMB may reveal about the breaking of fundamental discrete symmetries in the early universe. We have reviewed the present constraints, due to WMAP, for the cases of a hinted low resolution Parity anomaly as well as for cosmic birefringence. For the latter, the QUaD dataset has provided the most stringent limits to date. We have also presented *Planck* forecasts. *Planck* may be able to confirm or deny the existence of the low resolution Parity anomaly. Moreover, it is expected to greatly improve the knowledge of the polarization pattern of the CMB. *Planck* will also probe photon birefringence, improving the present constraints by over an order of magnitude.

* * *

We acknowledge the use of the BCX and SP6 at CINECA under the agreement INAF/CINECA and the use of computing facility at NERSC. We acknowledge use of the HEALPix [76] software and analysis package for deriving the results in this paper. We acknowledge the use of the LAMBDA. Support for LAMBDA is provided by the NASA Office of Space Science. Work supported by ASI through ASI/INAF Agreement I/072/09/0 for the Planck LFI Activity of Phase E2.

REFERENCES

[1] Tauber J. *et al.*, *Astron. Astrophys.*, **520** (2010) A1.
[2] Bersanelli M. *et al.*, *Astron. Astrophys.*, **520** (2010) A4.
[3] Lamarre J. M. *et al.*, *Astron. Astrophys.*, **520** (2010) A9.
[4] Dupac X. and Tauber J., *A&A*, **430** (2005) 363.
[5] Mandolesi N. *et al.*, *Astron. Astrophys.*, **520** (2010) A3.
[6] Planck Collaboration *et al.*, arXiv:1101.2022 [astro-ph.IM].
[7] Planck HFI Core Team *et al.*, arXiv:1101.2039 [astro-ph.IM].
[8] Mennella A. *et al.*, arXiv:1101.2038 [astro-ph.CO].
[9] Planck Collaboration *et al.*, arXiv:1101.2023 [astro-ph.IM].
[10] Planck HFI Core Team *et al.*, arXiv:1101.2048 [astro-ph.CO].
[11] Zacchei A. *et al.*, arXiv:1101.2040 [astro-ph.IM].
[12] Planck Collaboration *et al.*, arXiv:1101.2037 [astro-ph.GA].
[13] Planck Collaboration *et al.*, arXiv:1101.2036 [astro-ph.GA].
[14] Planck Collaboration *et al.*, arXiv:1101.2034 [astro-ph.GA].
[15] Planck Collaboration *et al.*, arXiv:1101.2035 [astro-ph.GA].
[16] Planck Collaboration *et al.*, arXiv:1101.2032 [astro-ph.GA].
[17] Planck Collaboration *et al.*, arXiv:1101.2031 [astro-ph.GA].
[18] Planck Collaboration *et al.*, arXiv:1101.2029 [astro-ph.GA].
[19] Planck Collaboration *et al.*, arXiv:1101.2047 [astro-ph.GA].
[20] Planck Collaboration *et al.*, arXiv:1101.2046 [astro-ph.CO].
[21] Planck Collaboration *et al.*, arXiv:1101.2045 [astro-ph.CO].
[22] Planck Collaboration *et al.*, arXiv:1101.2044 [astro-ph.CO].

[23] Planck Collaboration *et al.*, arXiv:1101.1721 [astro-ph.CO].
[24] Planck Collaboration *et al.*, arXiv:1101.2028 [astro-ph.CO].
[25] Planck Collaboration *et al.*, arXiv:1101.2043 [astro-ph.CO].
[26] Planck Collaboration *et al.*, arXiv:1101.2027 [astro-ph.CO].
[27] Planck Collaboration *et al.*, arXiv:1101.2026 [astro-ph.CO].
[28] Planck Collaboration *et al.*, arXiv:1101.2025 [astro-ph.CO].
[29] Planck Collaboration *et al.*, arXiv:1101.2024 [astro-ph.CO].
[30] Planck Collaboration *et al.*, arXiv:1101.2041 [astro-ph.CO].
[31] Larson D. *et al.*, arXiv:1001.4635 [astro-ph.CO].
[32] Komatsu E. *et al.*, *Astrophys. J. Suppl.*, **192** (2011) 18.
[33] Copi C. J., Huterer D., Schwarz D. J. and Starkman G. D., arXiv:1004.5602 [astro-ph.CO].
[34] Bennett C. L. *et al.*, arXiv:1001.4758 [astro-ph.CO].
[35] Copi C. J., Huterer D., Schwarz D. J., Starkman G. D., *Phys. Rev. D*, **75** (2007) 023507.
[36] Copi C. J., Huterer D., Schwarz D. J. and Starkman G. D., *Mon. Not. Roy. Astron. Soc.*, **399** (2009) 295.
[37] Eriksen H. K., Banday A. J., Gorski K. M., Hansen F. K. and Lilje P. B., *Astrophys. J.*, **660** (2007) L81.
[38] Hansen F. K., Banday A. J., Gorski K. M., Eriksen H. K. and Lilje P. B., *Astrophys. J.*, **704** (2009) 1448.
[39] Hoftuft J., Eriksen H. K., Banday A. J., Gorski K. M., Hansen F. K. and Lilje P. B., *Astrophys. J.*, **699** (2009) 985.
[40] Eriksen H. K., Hansen F. K., Banday A. J., Gorski K. M. and Lilje P. B., *Astrophys. J.*, **605** (2004) 14; **609** (2004) 1198 (E).
[41] Paci F., Gruppuso A., Finelli F., Cabella C., De Rosa A., Mandolesi N. and Natoli P., *Mon. Not. Roy. Astron. Soc.*, **407** (2010) 399.
[42] Pietrobon D., Cabella P., Balbi A., Crittenden R., de Gasperis G. and Vittorio N., *Mon. Not. Roy. Astron. Soc. Lett.*, **402** (2009) L34.
[43] Vielva P., Martinez-Gonzalez E., Barreiro R. B., Sanz J. L. and Cayon L., *Astrophys. J.*, **609** (2004) 22.
[44] Tegmark M., de Oliveira-Costa A. and Hamilton A., *Phys. Rev. D*, **68** (2003) 123523.
[45] Copi C. J., Huterer D. and Starkman G. D., *Phys. Rev. D*, **70** (2004) 043515.
[46] Schwarz D. J., Starkman G. D., Huterer D. and Copi C. J., *Phys. Rev. Lett.*, **93** (2004) 221301.
[47] Weeks J. R., arXiv:astro-ph/0412231.
[48] Land K. and Magueijo J., *Phys. Rev. Lett.*, **95** (2005a) 071301.
[49] Abramo L. R., Bernui A., Ferreira I. S., Villela T. and Wuensche C. A., *Phys. Rev. D*, **74** (2006) 063506.
[50] Wiaux Y., Vielva P., Martinez-Gonzalez E. and Vandergheynst P., *Phys. Rev. Lett.*, **96** (2006) 151303.
[51] Vielva P., Wiaux Y., Martínez-González E., Vandergheynst P., *Mon. Not. R. Astron. Soc.*, **381** (2007) 932.
[52] Gruppuso A. and Gorski K. M., *J. Cosmol. Astropart. Phys.*, **1003** (2010) 019.
[53] Gruppuso A. and Burigana C., *J. Cosmol. Astropart. Phys.*, **0908** (2009) 004.
[54] Bernui A. and Reboucas M. J., *Phys. Rev. D*, **81** (2010) 063533.
[55] Bernui A., Reboucas M. J. and Teixeira A. F. F., arXiv:1005.0883 [astro-ph.CO].
[56] Cruz M., Martinez-Gonzalez E., Vielva P. and Cayon L., *Mon. Not. Roy. Astron. Soc.*, **356** (2005) 29.
[57] Cruz M., Martinez-Gonzalez E. and Vielva P., arXiv:0901.1986 [astro-ph]
[58] Land K. and Magueijo J., *Phys. Rev. D*, **72** (2005) 101302.
[59] Kim J. and Naselsky P., *Astrophys. J.*, **714** (2010a) L265.
[60] Kim J. and Naselsky P., (2010b) arXiv:1002.0148 [astro-ph.CO].

[61] Gruppuso A., Finelli F., Natoli P., Paci F., Cabella P., De Rosa A. and Mandolesi N., *Mon. Not. Roy. Astron. Soc.*, **411** (2011) 3.
[62] Lenhnert R., hep-ph/0611177.
[63] Greenberg O. W., *Phys. Rev. Lett.*, **89** (2002) 231602.
[64] Greenberg O. W., *Found. Phys.*, **36** (2006) 1535.
[65] Bluhm R., hep-ph/0112318.
[66] Mewes M., hep-ph/0307161.
[67] Amelino-Camelia G. *et al.*, *Nature*, **393** (1998) 763.
[68] Carroll S. M., Field G. B. and Jackiw R., *Phys. Rev. D*, **41** (1990) 1231.
[69] Carroll S. M. and Field G. B., *Phys. Rev. D*, **43** (1991) 3789.
[70] Leach S. M. *et al.*, *Astron. Astrophys.*, **491** (2008) 597.
[71] Zaldarriaga M., *Astrophys. J.*, **503** (1998) 1 [arXiv:astro-ph/9709271].
[72] Zaldarriaga M. and Seljak U., *Phys. Rev. D*, **55** (1997) 1830.
[73] Tegmark M., *Phys. Rev. D*, **55** (1997) 5895.
[74] Tegmark M. and de Oliveira-Costa A., *Phys. Rev. D*, **64** (2001) 063001.
[75] Gruppuso A., de Rosa A., Cabella P., Paci F., Finelli F., Natoli P., de Gasperis G. and Mandolesi N., *Mon. Not. Roy. Astron. Soc.*, **400** (2009) 1.
[76] Gorski K. M., Hivon E., Banday A. J., Wandelt B. D., Hansen F. K., Reinecke M. and Bartelmann M., HEALPix: A Framework for High-resolution Discretization and Fast Analysis of Data Distributed on the Sphere, *Astrophys. J.*, **622** (2005) 759.
[77] Jarosik N. *et al.* [WMAP Collaboration], *Astrophys. J. Suppl.*, **170** (2007) 263.
[78] Dunkley J. *et al.* (WMAP), *Astrophys. J. SS*, **180** (2009) 306.
[79] Scannapieco E. S. and Ferreira P. G., *Phys. Rev. D*, **56** (1997) 7493.
[80] Pogosian L., Vachaspati T. and Winitzki S., *Phys. Rev. D*, **65** (2002) 083502.
[81] Giovannini M., *Phys. Rev. D*, **71** (2005) 021301.
[82] Lue A., Wang L. and Kamionkowski M., *Phys. Rev. Lett.*, **83** (1999) 1506.
[83] Saito S., Ichiki K. and Taruya A., arXiv:0705.3701, 2007.
[84] Maity D., Majumdar P., SenGupta S., *J. Cosmol. Astropart. Phys.*, **0406** (2004) 005.
[85] Lepora N. F., gr-qc/9812077, 1998.
[86] Balaji K. R. S., Brandenberger R. H. and Easson D. A., *J. Cosmol. Astropart. Phys.*, **12** (2003) 008.
[87] Cabella P., Natoli P. and Silk J., *Phys. Rev. D*, **76** (2007) 123014.
[88] Davoudiasl H. *et al.*, *Phys. Rev. Lett.*, **93** (2004) 201301.
[89] Li H., Li M. and Zhang X., *Phys. Rev. D*, **70** (2004) 047302.
[90] Carroll S. M. and Field G. B., *Phys. Rev. Lett.*, **79** (1997) 2394.
[91] Carroll S. M., *Phys. Rev. Lett.*, **81** (1998) 3067.
[92] Nodland B. and Ralston J. P., *Phys. Rev. Lett.*, **78** (1997) 3043.
[93] Eisenstein D. J. and Bunn E. F., *Phys. Rev. Lett.*, **79** (1997) 1957.
[94] Leahy J. P., astro-ph/9704285, 1997.
[95] Feng B., Li H., Li M., Zhang X., *Phys. Lett. B*, **620** (2005) 27.
[96] Wu E. Y. S. *et al.* [QUaD Collaboration], *Phys. Rev. Lett.*, **102** (2009) 161302.
[97] Xia J. Q., Li H., Zhao G. B. *et al.*, *Int. J. Mod. Phys. D*, **17** (2009) 2025.
[98] Pagano L. *et al.*, *Phys. Rev. D*, **80** (2009) 043522.